Effects of systematic shortening of noncovalent C8 side chain on the cytotoxicity and NF-κB inhibitory capacity of pyrrolobenzodiazepines (PBDs)

Article (Published Version)

Journal of Medicinal Chemistry

Article

Cite This: J. Med. Chem. 2019, 62, 2127−2139

pubs.acs.org/jmc

Effects of Systematic Shortening of Noncovalent C8 Side Chain on the Cytotoxicity and NF-κB Inhibitory Capacity of Pyrrolobenzodiazepines (PBDs)

David B. Corcoran,[†] Thomas Lewis,[‡] Kazi S. Nahar,[†] Shirin Jamshidi,[†] Christopher Fegan,[‡] Chris Pepper,[‡,§] David E. Thurston,*[,†] and Khondaker Miraz. Rahman*[,†]

[†]Institute of Pharmaceutical Science, School of Cancer and Pharmaceutical Sciences, King's College London, London SE1 9NH, U.K.

[‡]School of Medicine, Cardiff University, Cardiff CF14 4XN, U.K.

[§]Brighton and Sussex Medical School, University of Sussex, Brighton BN1 9PX, U.K.

Supporting Information

ABSTRACT: The systematic shortening of the noncovalent element of a C8-linked pyrrolobenzodiazepine (PBD) conjugate (**13**) led to the synthesis of a 19-member library of C8-PBD monomers. The critical elements of **13**, which were required to render the molecule cytotoxic, were elucidated by an annexin V assay. The effects of shortening the noncovalent element of the molecule on transcription factor inhibitory capacity were also explored through an enzyme-linked immunosorbent assay-based measurement of nuclear NF-κB upon exposure of JJN-3 cells to the synthesized molecules. Although shortening the noncovalent interactive element of **13** had a less than expected effect upon compound cytotoxicity due to reduced DNA interaction, the transcription factor inhibitory capacity of the molecule was notably altered. This study suggests that a relatively short noncovalent side chain at the C8 position of PBD is sufficient to confer cytotoxicity. The shortened PBD monomers provide a new ADC payload scaffold because of their potent cytotoxicity and drug-like properties.

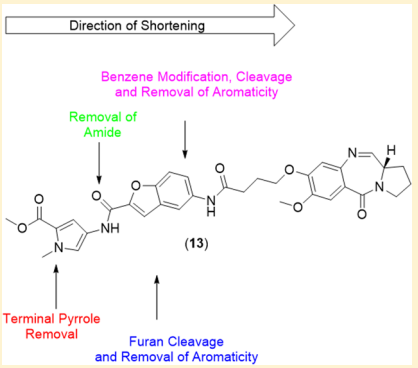

INTRODUCTION

Since their discovery in *Streptomyces* bacteria over half a century ago, pyrrolo[2,1-*c*][1,4]benzodiazepine (PBD) structures have been of interest as possible chemotherapeutic agents. This is due to their ability to sequence selectively bind covalently to DNA, to cause DNA strand cleavage, and to inhibit DNA-associated enzymes.[1−3] Two critical features of the PBD structure confer this covalent binding capacity on the molecule. S stereochemistry at the C11*a* position of the molecule bestows a right-handed longitudinal twist upon the structure, allowing an effective fit along the minor groove of the DNA helix.[4,5] Complementing this optimal fit is the presence of an interconvertible imine-carbinolamine moiety at the N10−C11 position of the molecule. This electrophilic center undergoes attack from the C2−NH_2 of guanine bases in the minor groove, forming the covalent aminal bonds responsible for their potent cytotoxicity[6−8] (Figure 1A).

PBD structures have been found to form covalent bonds with some guanines in the DNA minor groove more frequently than others, particularly those flanked by purine bases,[5,9] although more recent data suggest kinetic preferences when guanines are flanked by pyrimidines.[10] This potential for relative selectivity of binding is of interest, given that the pathogenesis of many cancers is associated with the aberrant binding of transcription factors, such as nuclear factor kappa B (NF-κB), to sequence-specific promoter regions of DNA.[11−15] The conjugation of subunits, capable of noncovalent interactions with DNA bases, to the C8 position of the PBD structure (via a carbon linker of variable length) has led to the development of hybrid molecules that can interact selectively with longer sequences of DNA than the typical purine−guanine−purine motifs of unmodified PBD structures. Such molecules have shown a capacity to inhibit the binding of transcription factors, such as NF-Y[16] and NF-κB[17] to their respective promoter sequences. More recent C8-modified PBDs, such as KMR-28-39 (Figure 1B) synthesized by Rahman and co-workers[18] have demonstrated the evidence of preclinical activity of such PBD conjugates. In addition to their cytotoxicity and anti-tumor activity, PBD-heterocyclic hybrids have shown significant antimicrobial activity.[19−21] More recently, PBDs are being used as cytotoxic payloads for antibody−drug conjugates, and a number of these are currently undergoing clinical evaluation.[22]

Although the addition of noncovalent interactive subunits to the C8 position of PBD structures has been associated with the down-regulation of genes downstream of transcription factor activity,[17,18,23,24] the relationship between the structural

Received: November 27, 2018
Published: January 28, 2019

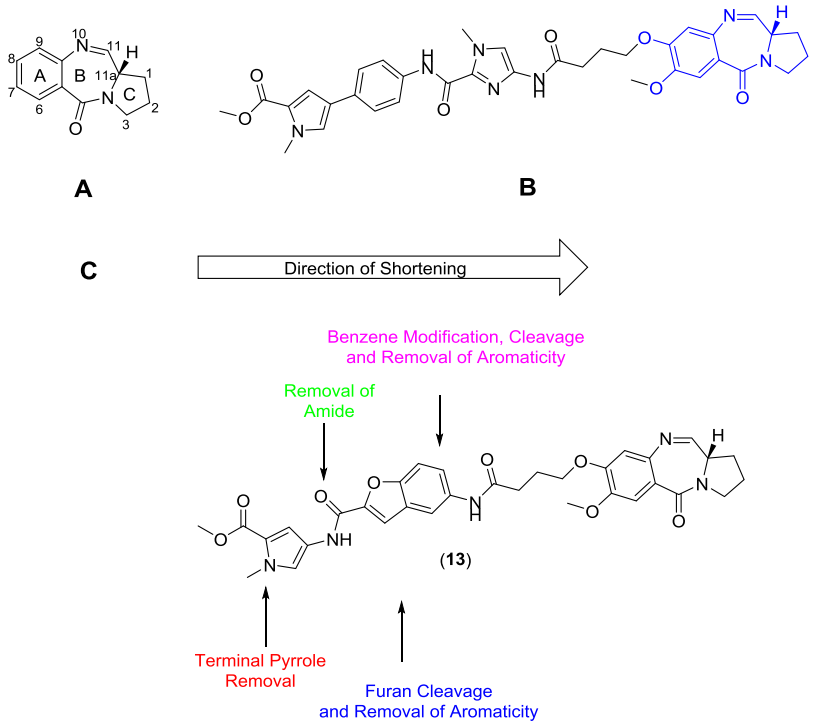

Figure 1. (A), The three-ring structure of the PBD core, with key atoms labelled. (B), The structure of KMR-28-39, with the PBD component highlighted in blue. (C), The shortening strategy for **13**, which underpinned the development of the novel PBD hybrids, is detailed in this paper.

Scheme 1. Conjugation of the Non-Covalent Element of the PBD Hybrid and Activation of the N10−C11 Imine

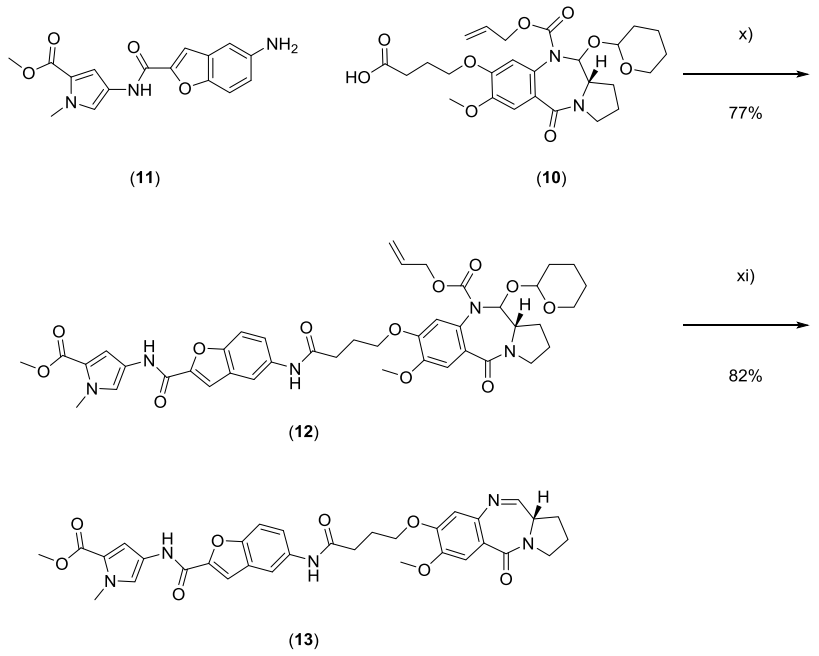

x) EDCI, DMAP, DMF, xi) tetrakis(triphenylphosphine)palladium(0), pyrrolidine, DCM

requirements and the potent cytotoxicity observed for these molecules has not been fully elucidated. The extent of C8 diversification required to confer this transcription factor activity (i.e., the core noncovalent interactive pharmacophore) remains unclear. In this paper, we investigated some of these uncertainties through the systematic shortening of a C8-linked monomer (**13**, Figure 1C) containing a pyrrole−benzofuran motif which has been previously explored in both noncovalent distamycin[25] and covalent duocarmycin analogues[26] and the subsequent generation of a library of 19 C8-linked PBD monomers. The effect of the reduction of the noncovalent element of the hybrid on both transcription factor activity and overall cytotoxicity was then evaluated.

DOI: 10.1021/acs.jmedchem.8b01849
J. Med. Chem. 2019, 62, 2127−2139

Table 1. Evaluation of the C8 Hybrid 13 and Its Shortened Derivatives in Primary CLL Cells and JJN-3 Cell Lines[a]

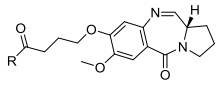

General PBD Core Structure

Name	R =	LC_{50} (nM)	
		Primary CLL	JJN-3 Cell Line
GWL-78	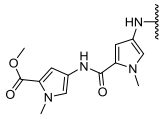	39	21
13	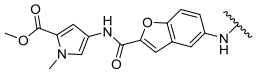	7.5	30
14	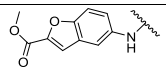	8.9	49
15	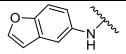	9.4	44
16	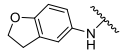	5.1	14.7
17	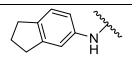	7.7	30
18	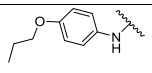	8.5	8.7
19	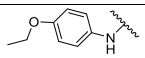	5.8	15.6
20	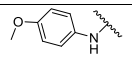	8.9	15.3
21	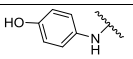	5500	2200
22	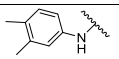	8.6	23.7
23	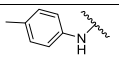	12.3	17.5
24	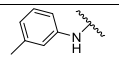	13.6	20.2
25	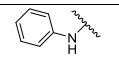	11.6	26.4
26	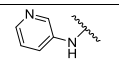	4200	1600
27	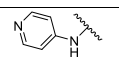	4900	6700
28	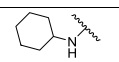	7100	1400
29	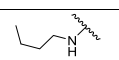	22400	51600
30	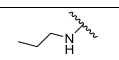	25100	12700
31	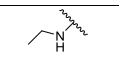	11700	28700
32	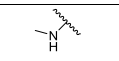	16100	18500

[a]LC_{50} values were calculated from sigmoidal dose−response curves generated from three independent experiments, performed in duplicate.

RESULTS AND DISCUSSION

Synthesis of PBD Hybrids. The PBD core (N10-Alloc, C11-THP protected) of the hybrids (**10**) was synthesized from vanillin, as previously described in the literature[18] (see the Supporting Information for scheme). A four-carbon linker was used to connect the PBD component with the noncovalent interactive subunits, as chains of this length had proven optimal for DNA binding in previous hybrid SAR studies. The linker was located at the C8 position of the molecule to allow an isohelical fit of the noncovalent component of the hybrid along the minor groove upon covalent PBD binding.[2]

After the synthesis of the PBD core, the C8 hybrid **13** was constructed using a combination of a benzofuran and an *N*-methyl pyrrole moiety. This was based upon the molecular structures of the side chains of KMR-28-39 (Figure 1B) and other molecules recently described by Basher and co-workers.[27] These benzofuran−pyrrole components were linked via Steglich amide bond formation at positions that maintained the overall fit of the hybrid for the DNA minor groove (i.e., C2/C5 for benzofuran, C1/C4 for *N*-methyl pyrrole components). The full synthesis of the noncovalent interactive hybrid component of **13** is summarized in the Supporting Information, with the conjugation to the PBD moiety and activation of the N10−C11 imine component of the molecule detailed in Scheme 1. A total of 19 new PBDs were synthesized by the systematic shortening of the noncovalent interactive element of **13** (Table 1). This process was analogous to the synthesis of **13**, with component **11**, replaced with designed building blocks to afford progressively shortened C8-PBDs.

Biological Evaluation. *Cytotoxicity Screening.* Given the established inhibition of the activity of the NF-κB transcription factor by previous (structurally similar) C8-linked PBD monomers, such as those described by Rahman and co-workers,[18] it was hypothesized that compound **13** and its shortened derivatives could share such properties. Accordingly, the initial screening of the compounds was carried out in primary tumor samples and a malignant cell line known to manifest aberrant activity of NF-κB. The pathogenesis of both chronic lymphocytic leukemia (CLL) and multiple myeloma has been linked to aberrant gene expression mediated, at least in part, by NF-κB.[28−33] Primary tissues were obtained from CLL patients (n = 3) with their informed consent, and the authenticated multiple myeloma cell line, JJN-3, was purchased from DSMZ (Germany). The compounds were added to cultures of the primary CLL cells and JJN-3 cells at concentrations between 1 nM and 100 μM in both primary leukemic cells and the cell line for 48 h. An annexin V binding assay was used to measure cytotoxicity, and LC_{50} values were calculated from the sigmoidal dose−response curves using

DOI: 10.1021/acs.jmedchem.8b01849
J. Med. Chem. 2019, 62, 2127−2139

Prism 6.0 software. A previously synthesized C8-linked PBD hybrid featuring transcription factor inhibitory properties, GWL-78,[34] was also evaluated as a positive control. The results of this cytotoxicity evaluation are described in Table 1, with the cytotoxicity dose−response curves obtained for each molecule detailed in the Supporting Information.

Prior to the screening of the shortened compound library in the CLL and JJN-3 cell cultures, it was expected that molecular shortening of the side chain of **13** would diminish compound activity. This was based upon the hypothesis that both the overall affinity of the PBD hybrid for DNA and the length of DNA sequences bound by the compound would be reduced because of the reduction in noncovalent interactions between the DNA minor groove and the C8 side chain of the molecule. This concept has been reflected in the cytotoxicity of previously synthesized PBD hybrids, which featured short C8-conjugated moieties. Such compounds either lacked notable cytotoxicity or were less cytotoxic than their longer side-chain counterparts. Examples of these compounds include a PBD hybrid containing a single pyrrole element synthesized by Borgatti and co-workers, as well as hybrids of similar structure by Thurston and co-workers, which were only weakly cytotoxic.[34,35]

The cytotoxicity of the compounds in the primary CLL cells and the JJN-3 cell line was therefore unexpected. For several of the compounds tested, LC_{50} values were obtained in the low nanomolar range, with good concordance in cytotoxicity observed between the primary CLL cells and the myeloma cell line. In total, 10 compounds maintained or improved activity with respect to **13** upon side chain shortening in primary CLL cells.

The cellular screen provided some insight into the structural features of the noncovalently interactive C8 side chain of **13** which may prove integral to its cytotoxic activity. It appeared that the presence of the terminal pyrrole moiety of **13** is not essential for its activity, as cytotoxicity was largely preserved for the benzofuran-containing compounds **14** and **15**. Aromaticity of the furan component of the benzofuran structure also appeared not to be crucial for its cytotoxicity. Indeed, the dihydrobenzofuran-containing compound, **16**, was one of the most cytotoxic compounds tested in primary CLL cells. Opening this furan ring also maintained activity at low nanomolar levels in both primary CLL cells and the JJN-3 cell line.

The importance of the oxygen moiety of benzofuran is less clear from this cellular evaluation. Replacement of the oxygen atom with a carbon (**17**) or its complete elimination (**22**−**24**) had little effect upon compound activity. This indicates that the potential hydrogen bond acceptor role of the oxygen plays little part in the overall cytotoxicity of **13**. Interestingly, reduced cytotoxicity was observed for **21**. In this case, the benzofuran oxygen is present as part of a phenol, rather than an ether functional group. The phenol moiety of **21** may act as a hydrogen bond donor, in contrast to its ether-containing analogues. The latter of these characteristics appeared to have an important effect on overall cytotoxicity.

Interestingly, the entire removal of the furan ring of the benzofuran side-chain component (**25**) failed to appreciably reduce the cytotoxicity. However, alterations to the benzene element of the benzofuran had more significant effects upon cytotoxicity. The introduction of a nitrogen atom into the ring, through the use of aminopyridine building blocks, eliminated compound activity at the dose range tested. Such a deleterious effect upon compound activity was unexpected. In a similar fashion to the introduction of the phenol group in **21**, the nitrogen of the pyridine ring may ionize depending upon the pH conditions. In a mildly acidic environment, the pyridine ring is protonated (pK_a of the conjugate acid is around 5.72), creating a formal positive charge. This charge may affect the ability of the molecule to penetrate the cell membrane and reach the minor groove of DNA. Moreover, the charged conjugate acid also conferred another hydrogen bond donor group on the molecule. One or both of these effects are likely to impact upon the activity of the PBD hybrids **26** and **27**, which showed approximately a three-log reduction in cytotoxicity when compared to **13**.

Removal of the aromaticity of this ring notably reduced the cytotoxicity. The cyclohexane and ring-opened derivatives (**28**−**32**) showed poor activity in both primary CLL cells and the JJN-3 cell line. It is possible that the spatial alteration of this portion of the side chain from a planar sp^2 hybridized structure to sp^3 derivative was responsible for this loss of activity. The removal of the delocalized electrons of the aromatic system may also have affected compound activity because of the removal of potential $\pi-\pi$ interactions with DNA bases.

Given the surprisingly similar cytotoxicity of **13** and its shortened derivatives in the CLL primary tissue and JJN-3 cell line evaluations, it was decided to conduct an evaluation of the shortened PBD hybrids versus their parent **13** in healthy age-matched B- and T-cell cultures. This would establish whether the cytotoxicity observed in the malignant cells was mirrored in non-malignant cells and whether a notional therapeutic index was apparent. Six shortened derivatives of **13**, which showed potent cytotoxicity in the initial CLL and JJN-3 cellular screens, were chosen for evaluation in the healthy cells: **14**, **15**, **18**, **19**, **20**, and **28**. Normal peripheral blood B-cells and T-cells, derived from three donors, were incubated with the seven compounds for 48 h at concentrations ranging from 1 nM to 100 μM. Subsequently, the cells were harvested by centrifugation, and apoptosis was quantified using an annexin V assay. The cytotoxicity dose−response curves obtained are detailed in the Supporting Information, with Table 2 listing the LC_{50} values obtained in both normal B- and T-cells, as well as the relative toxicity in these cells compared to primary CLL cells.

All of the compounds tested showed cytotoxicity ranging from 0.39 to 12.4 μM in both cell types. The compounds showed differential toxicity in the primary CLL cells compared to the normal B-cells and normal T-cells with notional therapeutic indices between 1 and 2 logs. The least potent

Table 2. LC_{50} Values of 13 and Its Shortened Derivatives with Calculated Therapeutic Indices Relative to Primary CLL Cell Cytotoxicity

compound	normal B-cell LC_{50} (nM)	normal T-cell LC_{50} (nM)	B-cell/CLL therapeutic index	T-cell/CLL TI therapeutic index
13	930	1700	124	226.7
14	410	2100	46.1	236
15	1400	3900	148.9	414.9
18	390	1100	45.9	129.4
19	750	3000	129.3	517.2
20	640	690	71.9	77.5
28	1700	12 400	0.24	1.74

DOI: 10.1021/acs.jmedchem.8b01849
J. Med. Chem. 2019, 62, 2127−2139

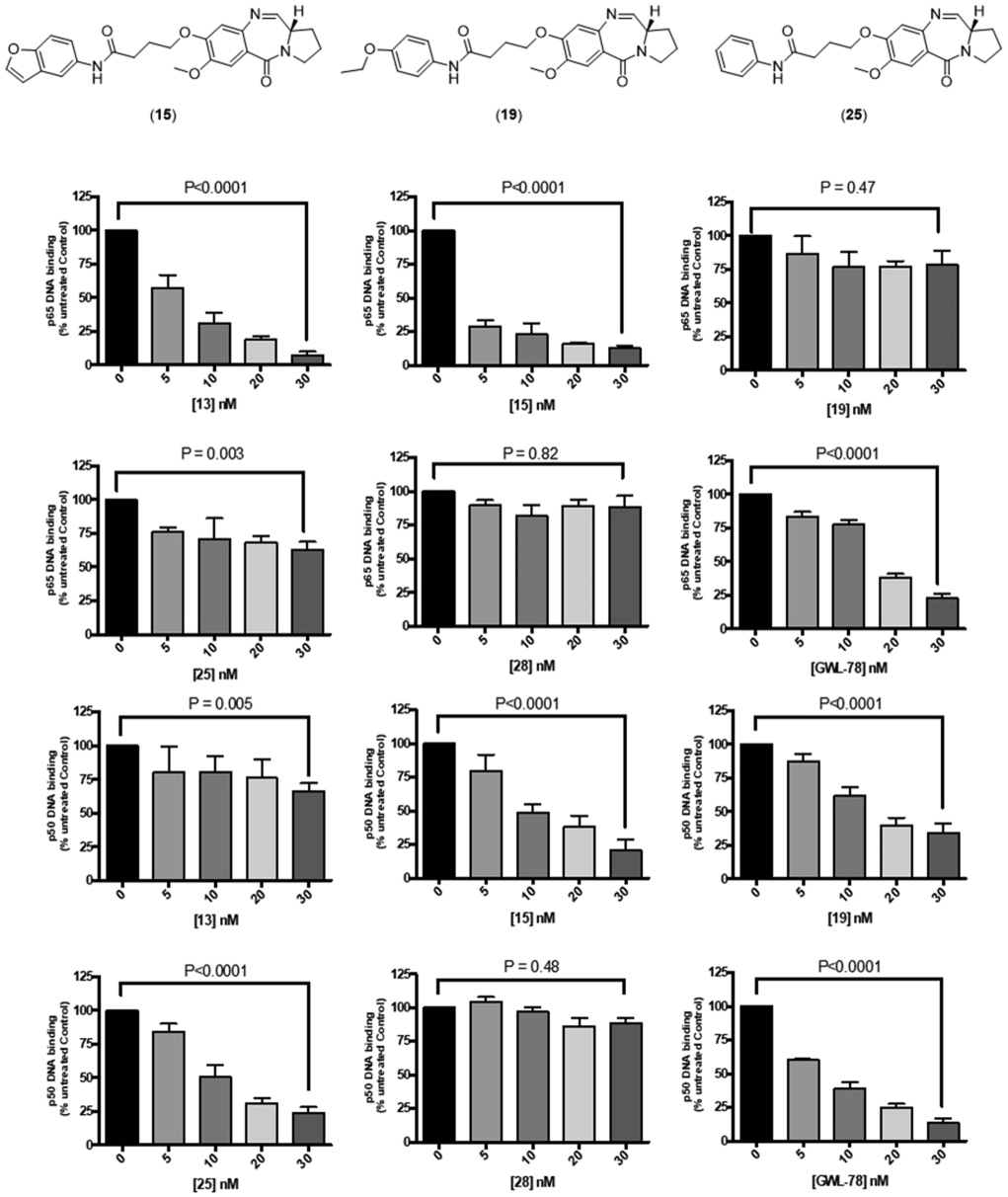

Figure 2. The effect of compounds **13**, **15**, **19**, **25**, **28** and GWL-78 on canonical NF-κB subunits after 4 h exposure.

compound tested, **28** showed no therapeutic index. Overall, the compounds showed better therapeutic indices against T-cells compared to B-cells with average therapeutic indices of 229.1 and 80.9, respectively. The observed therapeutic indices are large enough to consider further development of these C8-linked PBDs. However, there was no correlation between therapeutic indices and the length of the molecules. Essentially, this healthy cell evaluation confirmed that extensive shortening of the noncovalent component of **13** did little to affect either the cytotoxicity or selectivity profile of the compounds.

*Evaluation of the Effects of **13** and Derivatives on Nuclear Levels of NF-κB.* Given the lack of observable cytotoxicity differences between **13** and all but its most shortened C8-side-chain derivatives, it was decided to evaluate whether the reduction of the C8-linked noncovalent interactive side chain had any effect upon potential transcription factor inhibition by compound **13**.

The potent cytotoxicity observed for **13** and its derivatives in a number of NF-κB-dependent cancer cell types provided indirect evidence for their potential as possible inhibitors of this transcription factor. Moreover, the previously reported cellular inhibition by similar PBD hybrids of NF-κB[17,18,36] provided further impetus to directly measure the potential of these novel C8-linked PBD monomers to alter the nuclear levels of this transcription factor.

As a result, the effect of **13** and five of its shortened derivatives (**15**, **19**, **20**, **21**, and **25**), on nuclear levels of NF-κB in JJN-3 cells, was investigated. The derivative compounds were chosen because of their potency and to provide representative examples of the various stages of the shortening of the noncovalent interactive component of the compound. JJN-3 cell lines were chosen over the primary CLL cell samples for this analysis as the levels of nuclear NF-κB were more consistent in this cell line compared to primary tumor cells derived from different patients.

The measurement of the effects of the four compounds on nuclear levels of NF-κB involved the use of an adapted enzyme-linked immunosorbent assay (ELISA). Nuclear

DOI: 10.1021/acs.jmedchem.8b01849
J. Med. Chem. 2019, 62, 2127−2139

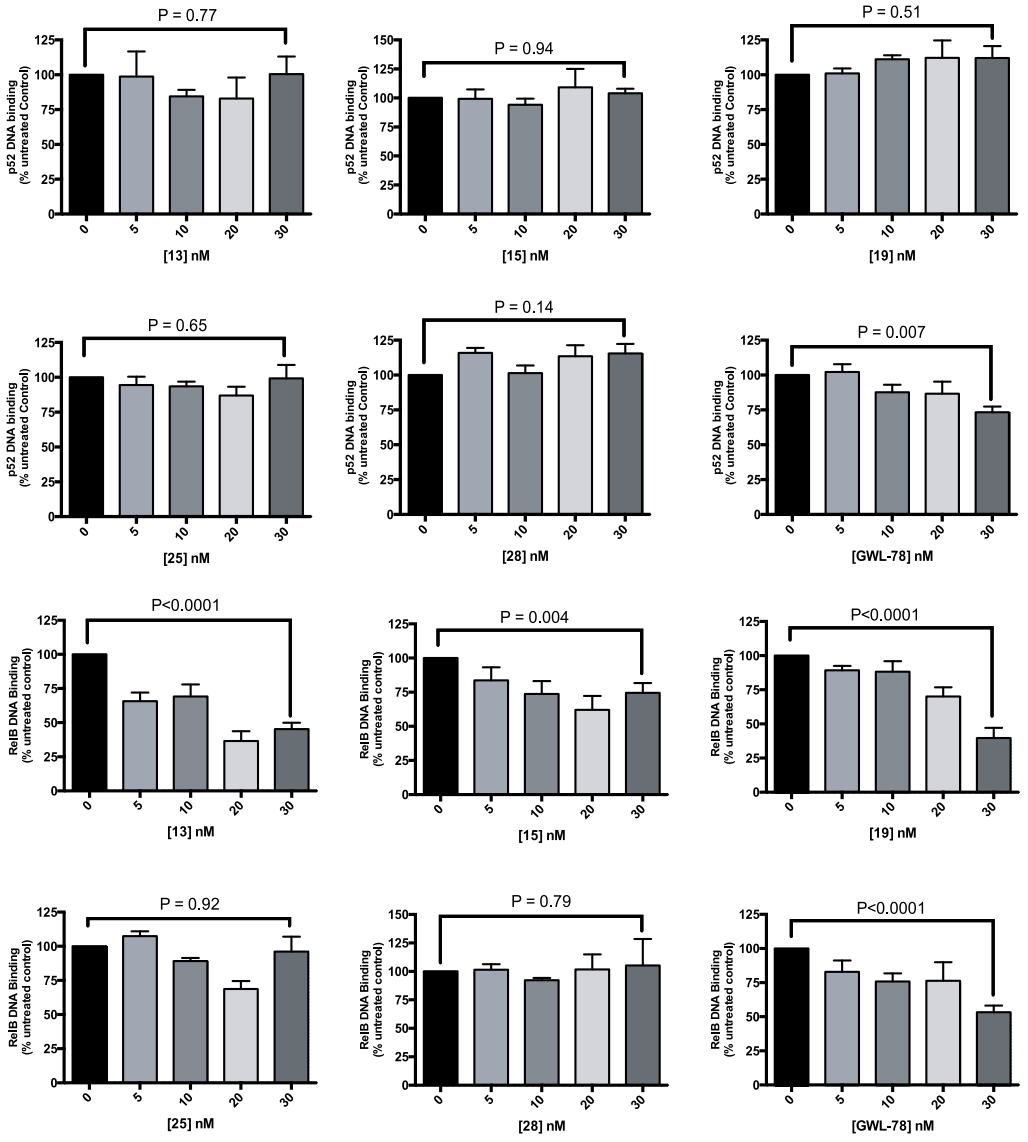

Figure 3. The effect of compounds **13**, **15**, **19**, **25**, **28** and GWL-78 on non-canonical NF-κB subunits after 4 h exposure.

extracts were prepared from treated and control cells using a nuclear extraction kit (Active Motif). Activated NF-κB subunits (p65, RelB, p52 or p50) in the samples were measured by oligonucleotide-based ELISA (Active Motif). Treated and control samples were incubated in the wells of a 96-well microtiter plate that were coated with the NF-κB consensus nucleotide sequence (5′-GGGACTTTCC-3′). NF-κB from the cell samples attached to the wells and was captured by specific antibody to either p65, RelB, p50 or p52. Binding of the specific NF-κB family member was then detected by an anti-rabbit-HRP-conjugated antibody. Developing solution was then added to the plate for 5 min prior to the addition of stop solution. The intensity of the developed color was proportional to the quantity of p65, RelB, p50 or p52 in each sample, and the amount of bound NF-κB was quantified (ng/μg nuclear extract) from subunit recombinant protein standard curves. The specificity of binding to the nucleotide sequence was ascertained by premixing free consensus nucleotide to the sample before adding the nuclear extract to the well. Sample determinations were normalized by the total cellular protein, as determined by the protein assay kit (Pierce). Data were expressed as a percentage of the untreated controls.

The quantified DNA binding activity for each NF-κB subunit in cells exposed to **13**, **15**, **19**, **20**, **21** and **25** was then related to a control value obtained from cells that had not been exposed to a PBD hybrid. The experiment was repeated in triplicate, and the effect of the compounds upon DNA binding of four subunits of NF-κB is illustrated in Figures 2 and 3 below. The c-Rel subunit was not evaluated in these experiments.

The evaluation of the effects on nuclear levels of NF-κB by the shortened PBD hybrids produced some interesting results. The significant knockdown of p65 by **15** aside, the shortened compounds tested produced no significant reductions in nuclear levels of the p65 subunit activity, despite their highly potent cytotoxicity in JJN-3 cells. When placed in the context of the role of NF-κB subunit function in carcinogenesis, this was an interesting outcome. p65 overexpression has been implicated in the progression of malignancy; a previous analysis of a cohort of CLL patient samples revealed significant up-regulation of the p65 subunit[28] and this was associated with disease progression.[37]

DOI: 10.1021/acs.jmedchem.8b01849
J. Med. Chem. 2019, 62, 2127−2139

The nuclear activity of p52 was unaffected or increased (**13** and **19**) by the PBD hybrids, whereas the RelB subunit was significantly decreased by **13**, but not by the shortened derivatives. Interestingly, all three of the shortened compounds tested significantly reduced p50 levels. This was not the case for **13**. However, the role of p50 in carcinogenesis is to date ill-defined,[38] and in some cases, increased levels of the subunit may promote apoptotic pathways.[39] Accordingly, the differential capacity of the PBD hybrids to inhibit the p65 subunit was considered in greater detail.

An evaluation of the structures of the three compounds (Figure 2) tested in this assay may help explain the differences in effect upon nuclear levels of NF-κB observed, especially the levels of p65. The parent **13** PBD hybrid molecule showed consistent inhibition of nuclear p65 activity. Compound **15**, which also significantly inhibited the p65 subunit, shares the greatest side chain similarity with **13** of the three compounds tested. The **15** side chain retains an intact benzofuran moiety common to its predecessors. This benzofuran is disrupted in **19** and **25**, with both the aromaticity and rigid cyclic structure of the furan ring of the benzofuran removed. Both compounds showed no discernible effect on nuclear p65 levels, despite their potency.

The results of this assay provided a more subtle insight into potential mechanisms of activity of PBD hybrids than a reliance on cell cytotoxicity assays alone. Although all of the compounds tested showed promising potency characteristics in a range of cancer cell lines, their NF-κB transcription factor inhibitory effects differed depending upon the side-chain composition. Compound **13**, containing the longest non-covalent interactive element, displayed the most effective inhibition of NF-κB and effects upon nuclear p65, and RelB levels appeared to diminish in tandem with the reduction of this element in the derivatives **15**, **19**, and **25** (although some increased inhibition of p50 was observed).

The clear differences in the NF-κB inhibitory capacity observed through the systematic shortening of **13** contrasted with the relatively comparable cytotoxicity profiles of all but the most shortened library derivatives. Two possible explanations may help explain this incongruity.

First, it is possible that the effects of the noncovalent interactive elements of the PBD hybrids on nuclear NF-κB activity are unrelated to their cytotoxic mechanism of activity. Such an assessment would regard the PBD monomers primarily as traditional DNA alkylating agents, with the transcription factor inhibitory effects (such as the p65 inhibition), displayed by molecules such as **13** effects, rather than the causes of PBD cytotoxicity. In this scenario, the noncovalent element of the molecules merely serves to confer different physicochemical properties on the compound or alter the nuclear penetration rate and extent of adduct formation with DNA.

The second, more compelling explanation for differences in the transcription factor inhibitory activity between PBD hybrids with varying noncovalent interactive elements is slightly more nuanced. Although all PBD molecules feature an ability to bind covalently to DNA and act to some extent as traditional alkylating agents, some may do so in a relatively more selective manner than others. It may be argued that the shortened derivatives of **13**, such as **25**, which feature short, low molecular weight side chains, bind to guanines along the minor groove indiscriminately. It is unlikely that such shortened structures (which form adducts spanning c. 4−5 DNA bases) would feature either the affinity or diameter to specifically disrupt conserved 8−9 base transcription factor promotor sequences. On the other hand, the presence of longer noncovalent interactive elements (such as those found in **13**) conjugated to PBD structures may subtly alter their binding distribution along the minor groove. By adding moieties capable of interacting noncovalently with DNA sequences in a relatively selective manner, the covalent adducts of PBD structures may be (to some extent) preferentially directed toward the longer, more specific sequences of DNA that are bound by transcription factors. Although the traditional effects of nonselective alkylation undoubtedly still occur, additional mechanisms of cell disruption (such as transcription factor inhibition) may also underpin the cytotoxicity of molecules such as **13**.

2D QSAR Analysis. A two-dimensional quantitative QSAR study of all compounds was carried out using a multiple linear regression (MLR) method to determine if there are any correlations between the biological activity ($1/LC_{50}$) and physicochemical descriptors log *P*, molecular weight, steric factors, and electronic factors. Leave-one-out cross validation was the regression method applied in the MLR model to study the correlation of the descriptors and the LC_{50} of the compounds. The results are listed in Table 3. The study showed slightly better correlation between the biological activity of the molecules in primary CLL cells (0.63) compared to JJN-3 cell lines (0.52). The correlation improved when only log *P* (0.74) or molecular weight (0.68) was considered in primary CLL cells. However, the correlations between biological activity in JJN-3 cell line and log *P* (0.58) or molecular weight (0.48) were moderate.

Table 3. 2D QSAR Parameters Showing Correlation between Biological Activity ($1/LC_{50}$) of PBD Hybrids in Primary CLL Cells and JJN-3 Cell Line and All Physiochemical Descriptors Determined Using MLR Model[a]

	primary CLL cells	JJN-3 cell line
RMSEcv	0.98	1.03
R^2 cv	0.63	0.53
RMSEc	0.50	0.47
R^2cal	0.88	0.87

[a]RMSEcv: root mean square errors of error for cross validation; R^2cv: regression coefficient for cross validation; RMSEc: root mean square errors of error for calibration; R^2cal: regression coefficient for calibration.

Molecular Modeling with DNA Sequences. As all of the compounds including the shortened compounds are expected to exert their cytotoxicity by covalent bonding with DNA and subsequent inhibition of transcription factors, a molecular modeling study was carried with four compounds (**13**, **20**, **23**, and **32**) with different C8 side-chain lengths and one AT-rich and one GC-rich DNA sequences. These compounds represent a mix of longer and shorter PBD compounds synthesized with a range of cytotoxicities. The molecular docking study suggested that all four compounds are able to snugly bind with the DNA minor groove and retain the shape characteristics required for the DNA minor groove binding molecules (Figures 4, S3 and S4). The energy of binding calculation showed the highest value for compound **13** with −11 KJ/mole for AT-rich DNA and −10.7 KJ/mol for the GC-rich DNA.

DOI: 10.1021/acs.jmedchem.8b01849
J. Med. Chem. 2019, 62, 2127−2139

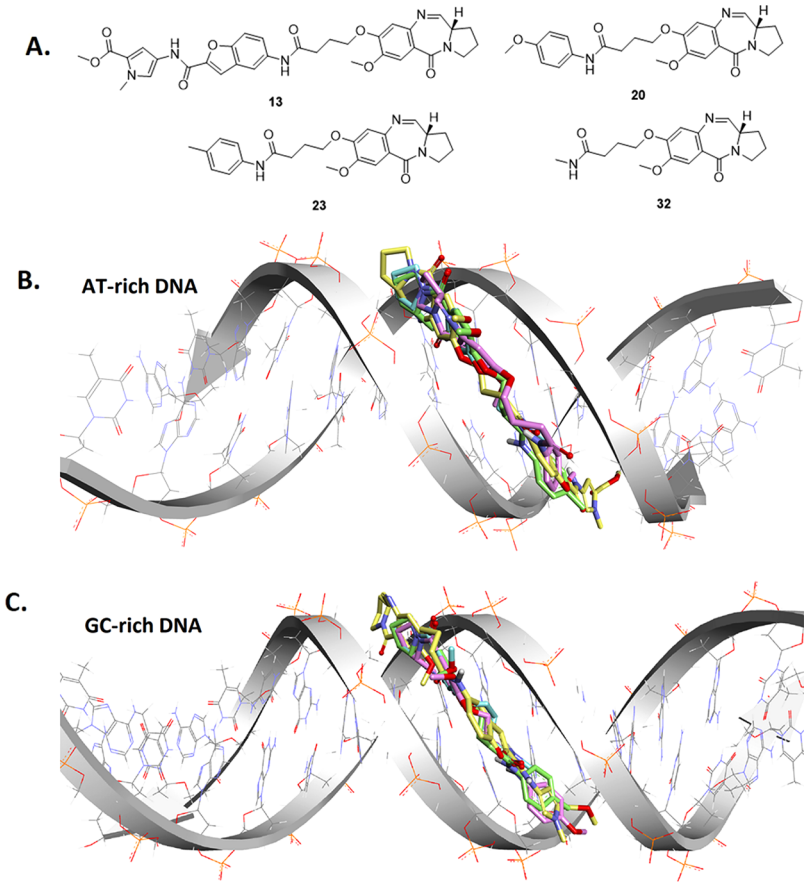

Figure 4. (A) The structures of the C8-PBD hybrids evaluated in the molecular modelling study; overlaid molecular docking images of PBD hybrids with (B) AT-rich and (C) GC-rich DNA sequences.

The values obtained for **20** and **23** were comparable, and the value for compound **32** was slightly lower (Table S1). The findings of the study broadly support the experimental observation as the shortened molecules retained their ability to interact with DNA sequences. However, the relative lack of activity of compound **32** cannot be explained by modeling alone as the physicochemical property of the molecule likely to have played an important role in the overall activity of the molecule.

CONCLUSIONS

The systemic shortening of the C8 side chain of PBD monomers show that transcription factor inhibitory effects may not necessarily translate into increased overall cytotoxicity or tolerability in vitro for PBD-type molecules. This observation may be useful in the design of monoalkylating PBD monomers that are currently being explored as standalone anticancer agents and payloads for antibody–drug conjugates. It is possible, however, that differential tolerability effects may only manifest themselves in in vivo evaluations. Indeed, the high therapeutic index of historical PBD hybrids (featuring longer noncovalent interactive elements of structure similar to that of **13**) versus unsubstituted PBD cores[39] provides the rationale for in vivo investigations of the novel PBD structures described in this paper. Such evaluations are currently underway.

EXPERIMENTAL SECTION

Synthesis. *General Material and Methods.* Synthetic building blocks, reagents, solvents, and chemicals were purchased from Sigma-Aldrich, Fluorochem, Fisher Scientific, Alfa Aesar, and Bachem, respectively. All reactions carried out were monitored by thin-layer chromatography carried out on E. Merck silica gel 60 F254 plates (0.25 mm). The plates were visualized using UV light at 254 nm and potassium permanganate staining where required. Purification using flash column chromatography was carried out using standard glass columns and silica gel as a stationary phase (Merck 60, 230–400 mesh ASTM). Where freeze drying of intermediates/final compounds was carried out, this was done using a Heto-Lyolab 3000 freeze dryer. High-performance liquid chromatography coupled to mass spectrometry was carried out on reaction mixtures, intermediates, and final products. This analysis was performed on a Waters Alliance 2695 separation system using water (solvent A) and acetonitrile (solvent B) as mobile phases using a Monolithic C18 50 × 4.60 mm column by phenomenex. UV detection was performed on a diode array detector. Formic acid was used to ensure acidic conditions throughout the analysis and was used at concentrations of 0.1%.

All of the compounds tested for their biological activity are >95% pure, confirmed with two different HPLC analysis methods. A 10 min (method A) and 5 min (method B) gradient was used to analyze submitted samples. The flow rate for both was 0.5 mL/min; 200 μL was split over a zero dead volume T piece which passed into the mass spectrometer. The wavelength range of the UV detector of the HPLC system was 220–400 nm. The function type used was a diode array (535 scans). The column type was a monolithic C18 50 × 4.60 mm column.

Method A (10 min run). 95% A 5% B for 2 min increasing to 50% B over 3 min. The gradient was then held at 50% B for 1 min and then increased to 95% B over 1.5 min. The quantity of B was then returned to 5% B over 1.5 min and held for 1 min.

Method B (5 min run). 95% A 5% B at 0 min increasing to 90% B over 3 min. The gradient was then increased to 95% B over 0.5 min

DOI: 10.1021/acs.jmedchem.8b01849
J. Med. Chem. 2019, 62, 2127–2139

and then held for 1 min. The quantity of B was then returned to 5% B over 0.5 min.

High-resolution mass spectrometry was undertaken on all final compounds synthesized. This was carried out using a Waters Micromass QTOF Global system in positive W-mode. Compounds were dissolved in DMSO at concentrations of 5 mM and introduced into the instrument using metal-coated borosilicate glass tips. ^{1}H NMR and ^{13}C NMR were carried out on a Bruker ADVANCE NMR spectrometer. The proton NMR was run at 400 Hz, whereas the carbon samples were run at 100 Hz. The temperature for all samples was 300 K. The spectra obtained for each sample were processed and analyzed using Topspin 3.0.

Synthesis of PBD Core, C8-Tails and C8-Linked PBD-Imines. PBD core **10** was synthesized following the literature procedure in nine steps in good yield. The intermediates were purified and fully characterized before progressing to the next step (Supporting Information).

*Synthesis of Methyl 4-(5-Aminobenzofuran-2-carboxamido)-1-methyl-1H-pyrrole-2-carboxylate (**11**).* 5-((*tert*-Butoxycarbonyl)-amino)benzofuran-2-carboxylic acid (0.5 g, 1.80 mmol) was dissolved in dimethylformamide (DMF) (3 mL). EDCI (0.70 g, 2 equiv) and DMAP (0.69 g, 2.5 equiv) were added to the reaction mixture, and the solution was stirred for 30 min. Methyl 4-amino-1-methyl-1*H*-pyrrole-2-carboxylate (0.40 g, 1.5 equiv) was then added to the flask, and the reaction mixture left overnight. After thin-layer chromatography (TLC) (20% ethyl acetate/DCM) and LC−MS showed completion of reaction, the reaction mixture was placed in ice water (30 mL) and extracted with ethyl acetate (3 × 50 mL). The ethyl acetate layers were combined and washed with citric acid solution (50 mL), bicarbonate solution (50 mL), water (50 mL), and brine (50 mL). The solution was concentrated in a rotary evaporator to yield brown oil. The crude material was briefly characterized by LC−MS before the Boc protected material was dissolved in methanol (1 mL for every mg of starting material), and 4 M HCl in dioxane (2 mL for every 25 mg of starting material). Gas evolution was observed. After 1 h, the reaction was found to be complete via LC−MS and TLC (20% ethyl acetate/DCM). The solution was concentrated using a rotary evaporator to yield the deprotected compound **11** as the hydrochloric acid salt in good yield (64% over two steps). ^{1}H NMR (400 MHz, $(CD_3)_2SO$): δ 10.87 (s, 1H), 10.14 (bs, 2H), 7.81 (d, 1H, J = 8.8 Hz), 7.76−7.74 (m, 2H) 7.55 (d, 1H, J = 1.2 Hz), 7.36 (dd, 1H, J = 1.6 Hz, 8.8 Hz), 7.03 (d, 1H, J = 1.2 Hz), 3.87 (s, 3H), 3.76 (s, 3H). EIMS (m/z): 314.0 $(M + H)^+$.

*Synthesis of Allyl (11aS)-7-methoxy-8-(4-((2-((5-(methoxycarbonyl)-1-methyl-1H-pyrrol-3-yl)carbamoyl)benzofuran-5-yl)-amino)-4-oxobutoxy)-5-oxo-11-((tetrahydro-2H-pyran-2-yl)oxy)-2,3,11,11a-tetrahydro-1H-benzo[e]pyrrolo[1,2-a][1,4]diazepine-10(5H)-carboxylate (**12**), and (S)-Methyl 4-(5-(4-((7-methoxy-5-oxo-2,3,5,11a-tetrahydro-1H-benzo[e]pyrrolo[1,2-a][1,4]diazepin-8-yl)oxy)butanamido)benzofuran-2-carboxamido)-1-methyl-1H-pyrrole-2-carboxylate (**13**).* **10** (0.132 g, 1.1 equiv) was dissolved in DMF (3 mL). EDCI (0.085 g, 2 equiv) and DMAP (0.071 g, 2.5 equiv) were added to the reaction mixture, and the solution was stirred for 30 min. **11** (0.07 g, 0.233 mmol) was then added to the flask, and the reaction mixture left overnight. After TLC (20% acetone/DCM)/LC−MS showed completion of reaction, the reaction mixture was placed in ice water (30 mL) and extracted with ethyl acetate (3 × 50 mL). The ethyl acetate layers were combined and washed with saturated citric acid solution (50 mL), bicarbonate solution (50 mL), water (50 mL), and brine (50 mL). The solution was concentrated in a rotary evaporator to yield brown oil. After characterization by LC−MS only, the protected intermediate **12** was then immediately deprotected to yield the imine. **12** (127 mg, 0.103 mmol) was dissolved in DCM (10 mL). To this solution, Tetrakis(triphenylphosphine)palladium(0) (6 mg, 0.08 equiv), triphenylphosphine (6.76 mg, 0.42 equiv), and pyrrolidine (10.93 μL, 2.0 equiv) were added. After approximately 30 min, the reaction was observed to go to completion by LC−MS and TLC (50% acetone/DCM) analysis. The solution was concentrated by rotary evaporation to remove the solvent and pyrrolidine and the crude immediately purified by flash column chromatography using a DCM/acetone mobile phase (75:25) yielding 100 mg **13** as a creamy white solid in 64% yield (two steps). ^{1}H NMR (400 MHz, $CDCl_3$): δ 8.74 (s, 1H), 8.62 (s, 1H), 7.86 (d, 1H, J = 2.0 Hz), 7.66 (d, 1H, J = 4.4 Hz), 7.51 (d, 1H J = 2.0 Hz), 7.48 (s, 1H), 7.44 (dd, 1H, J = 2.0, 9.2 Hz), 7.38, (s, 1H), 7.31 (s, 1H), 6.91, (d, 1H, J = 2.0 Hz), 6.81 (s, 1H), 4.10 (t, 2H, J = 6.0 Hz), 3.87 (s, 3H), 3.81 (s, 3H), 3.780 (s, 3H), 3.72−3.67 (m, 2H), 3.65−3.53 (m, 1H), 2.63−2.59 (m, 2H), 2.35−2.20 (m, 4H), 2.08−1.95 (m, 2H). ^{13}C NMR (100 MHz, $CDCl_3$): δ 171.2, 164.7, 162.7, 161.5, 155.8, 151.6, 150.5, 149.1, 147.6, 140.7, 134.4, 127.9, 121.4, 121.0, 120.7, 120.3, 120.0, 113.9, 111.7, 111.6, 110.8, 108.5, 68.1, 56.00, 53.8, 51.2, 50.7, 46.8, 36.9, 33.8, 29.6, 24.8, 24.2. HRMS m/z (+EI) calcd for $C_{33}H_{33}N_5O_8$ $(M)^+$, 628.2402; found, 628.2399. HPLC Method A: purity = >98%, retention time = 6.33 min. Method B: purity = >98% retention time = 3.25 min.

This general method was utilized for the synthesis of compounds **14**−**32**, with commercially available amino building blocks replacing **11**. Yields over two steps for each compound are detailed below. DCM/Acetone mobile phases were used during flash column purification of all of the compounds, with the proportion of acetone used depending upon the polarity of the compound.

*(S)-Methyl 5-(4-((7-Methoxy-5-oxo-2,3,5,11a-tetrahydro-1H-benzo[e]pyrrolo[1,2-a][1,4]diazepin-8-yl)oxy)butanamido)-benzofuran-2-carboxylate (**14**).* ^{1}H NMR (400 MHz, $CDCl_3$): δ 8.07 (d, 1H, J = 2.0 Hz), 7.81 (s, 1H), 7.67 (d, 1H, J = 4.4 Hz), 7.53 (s, 1H), 7.51 (s, 1H), 7.45 (s, 1H), 7.32 (dd, 1H, J = 2.0, 8.0 Hz), 6.84 (s, 1H), 4.25−4.14 (m, 2H), 3.98 (s, 3H), 3.86 (s, 3H), 3.86−3.78 (m, 1H), 3.73−3.67 (m, 1H), 3.61−3.54 (m, 1H), 2.68−2.62 (m, 2H), 2.34−2.28 (m, 4H), 2.10−2.04 (m, 2H). ^{13}C NMR (100 MHz, $CDCl_3$): δ, 171.0, 164.6, 162.6, 159.9, 152.5, 150.4, 147.6, 146.1, 140.7, 134.3, 127.3, 121.1, 120.5, 114.2, 112.4, 111.6, 110.8, 68.0, 56.1, 53.7, 52.4, 46.7, 34.0, 31.0, 29.7, 24.8, 24.2. HRMS m/z (+EI) calcd for $C_{27}H_{27}N_3O_7$ $(M)^+$, 506.1922; found, 506.1926. HPLC Method A: purity = >98%, retention time = 6.18 min. Method B: purity = >98%, retention time = 3.15 min. Yield = 52%, 67 mg (over two steps), pale brown solid.

*(S)-N-(Benzofuran-5-yl)-4-((7-methoxy-5-oxo-2,3,5,11a-tetrahydro-1H-benzo[e]pyrrolo[1,2-a][1,4]diazepin-8-yl)oxy)butanamide (**15**).* ^{1}H NMR (400 MHz, $CDCl_3$): δ 8.07 (s, 1H), 7.88 (d, 1H, J = 2.0 Hz), 7.64 (d, 1H, J = 4.4 Hz), 7.58 (d, 1H, J = 2.0 Hz), 7.49 (s, 1H), 7.38 (d, 1H, J = 8.8 Hz), 7.22 (dd, 1H, J = 2.0, 8.8 Hz), 6.81 (s, 1H), 6.69 (s, 1H), 4.19−4.08 (m, 2H), 3.84 (s, 3H), 3.82−3.75 (m, 1H), 3.69−3.65 (m, 1H), 3.59−3.51 (m, 1H), 2.62−2.58 (m, 2H), 2.30−2.23 (m, 4H), 2.05−2.01 (m, 2H). ^{13}C NMR (100 MHz, $CDCl_3$): δ 170.8, 164.6, 162.6, 151.9, 150.5, 147.7, 145.8, 140.7, 133.3, 127.7, 120.4, 117.7, 113.1, 111.6, 111.3, 110.8, 106.8, 68.0, 56.1, 53.7, 46.7, 33.9, 31.0, 24.9, 24.2. HRMS m/z (+EI) calcd for $C_{25}H_{25}N_3O_5$ $(M)^+$, 448.1867; found, 448.1871. HPLC Method A: purity = >98%, retention time = 6.07 min. Method B: purity = >98%, Rretention time = 3.10 min. Yield = 63%, 71 mg (over two steps), creamy white solid.

*(S)-N-(2,3-Dihydrobenzofuran-5-yl)-4-((7-methoxy-5-oxo-2,3,5,11a-tetrahydro-1H-benzo[e]pyrrolo[1,2-a][1,4]diazepin-8-yl)-oxy)butanamide (**16**).* ^{1}H NMR (400 MHz, $CDCl_3$): δ 7.69 (s, 1H), 7.67 (d, 1H, J = 4.4 Hz), 7.52 (s, 1H), 7.48 (s, 1H), 6.99 (dd, 1H, J = 2.0, 8.4 Hz), 6.83 (s, 1H), 6.69 (d, 1H, J = 8.4 Hz), 4.55 (t, 2H, J = 8.8 Hz), 4.19−4.11 (m, 2H), 3.88 (s, 3H), 3.85−3.78 (m, 1H), 3.73−3.67 (m, 1H), 3.61−3.54 (m, 1H), 3.18 (t, 2H, J = 8.8 Hz), 2.59−2.54 (m, 2H), 2.32−2.21 (m, 4H), 2.10−2.02 (m, 2H). ^{13}C NMR (100 MHz, $CDCl_3$): δ 170.6, 164.6, 162.6, 156.9, 150.4, 147.6, 140.7, 130.9, 127.5, 120.4, 118.4, 111.6, 110.7, 109.0, 71.4, 68.0, 56.1, 53.7, 46.7, 33.8, 31.8, 29.9, 29.6, 24.9, 24.2. HRMS m/z (+EI) calcd for $C_{25}H_{27}N_3O_5$ $(M)^+$, 450.2023; found, 450.2024. HPLC Method A: purity = >98%, retention time = 5.78 min. Method B: purity = >98%, retention time = 2.95 min. Yield = 60%, 69 mg (over two steps), transparent oil.

*(S)-N-(2,3-Dihydro-1H-inden-5-yl)-4-((7-methoxy-5-oxo-2,3,5,11a-tetrahydro-1H-benzo[e]pyrrolo[1,2-a][1,4]diazepin-8-yl)-oxy)butanamide (**17**).* ^{1}H NMR (400 MHz, $CDCl_3$): δ 7.71 (s, 1H), 7.66 (d, 1H, J = 4.4 Hz), 7.52 (s, 1H), 7.14−7.12 (m, 2H), 6.82 (s, 1H), 4.21−4.09 (m, 2H), 3.89 (s, 3H), 3.83−3.77 (m, 1H), 3.73−

DOI: 10.1021/acs.jmedchem.8b01849
J. Med. Chem. 2019, 62, 2127−2139

3.67 (m, 1H), 3.61−3.53 (m, 1H), 2.86 (q, 4H, 3.6, 16.8 Hz), 2.59−2.56 (m, 2H), 2.32−2.23 (m, 4H), 2.10−2.00 (m, 4H).). ^{13}C NMR (100 MHz, $CDCl_3$): δ 170.5, 164.6, 162.5, 150.4, 147.7, 145.1, 140.7, 140.2, 136.1, 124.4, 120.4, 118.1, 116.5, 111.5, 110.7, 67.9, 56.1, 53.7, 46.7, 34.0, 33.0, 32.3, 29.6, 25.6, 24.8, 24.2. HRMS *m/z* (+EI) calcd for $C_{26}H_{29}N_3O_4$ $(M)^+$, 448.2233; found, 448.2231. HPLC Method A: purity = >98%, retention time = 6.55 min. Method B: purity = >98%, retention time = 3.33 min. Yield = 63%, 72 mg (over two steps), creamy white solid.

*(S)-4-((7-Methoxy-5-oxo-2,3,5,11a-tetrahydro-1H-benzo[e]-pyrrolo[1,2-a][1,4]diazepin-8-yl)oxy)-N-(4-propoxyphenyl)-butanamide (**18**).* ^{1}H NMR (400 MHz, $CDCl_3$): δ 7.83 (s, 1H), 7.67 (d, 1H, *J* = 4.4 Hz), 7.52 (s, 1H), 7.38 (d, 2H, *J* = 9.2 Hz), 6.84 (s, 1H), 6.83 (d, 2H, *J* = 9.2 Hz), 4.19−4.10 (m, 2H), 3.89 (t, 2H, *J* = 6.4 Hz), 3.88 (s, 3H), 3.86−3.80 (m, 1H), 3.75−3.67 (m, 1H), 3.62−3.55 (m, 1H), 2.59−2.53 (m, 2H), 2.33−2.22 (m, 4H), 2.10−2.00 (m, 2H), 1.83−1.75 (sex, 2H, *J* = 7.2 Hz), 1.03 (t, 3H, *J* = 7.2 Hz). ^{13}C NMR (100 MHz, $CDCl_3$): δ 170.5, 164.6, 162.5, 155.9, 150.5, 147.7, 140.7, 132.1, 131.0, 128.6, 128.5, 121.8, 120.4, 114.7, 111.6, 110.8, 67.8, 68.0, 56.1, 46.7, 33.8, 29.6, 24.8, 24.2, 22.6, 10.5. HRMS *m/z* (+EI) calcd for $C_{26}H_{31}N_3O_5$ $(M)^+$, 466.2332; found, 466.2336. HPLC Method A: purity = >98%, retention time = 6.57 min. Method B: purity = >98%, retention time = 3.33 min. Yield = 65%, 77 mg (over two steps), pale orange solid.

*(S)-N-(4-Ethoxyphenyl)-4-((7-methoxy-5-oxo-2,3,5,11a-tetrahydro-1H-benzo[e]pyrrolo[1,2-a][1,4]diazepin-8-yl)oxy)butanamide (**19**).* ^{1}H NMR (400 MHz, $CDCl_3$): δ 7.84 (s, 1H), 7.64 (d, 1H, *J* = 4.4 Hz), 7.49 (s, 1H), 7.36 (d, 2H, *J* = 8.8 Hz), 6.80 (s, 1H), 6.80 (d, 2H, *J* = 8.8 Hz), 4.17−4.07 (m, 2H), 3.97 (q, 2H, *J* = 3.2 Hz), 3.84 (s, 3H), 3.82−3.76 (m, 1H), 3.71−3.67 (m, 1H) 3.59−3.52 (m, 1H) 2.54−2.51 (m, 2H), 2.33−2.20 (m, 4H), 2.08−1.97 (m, 2H), 1.37 (t, 3H, *J* = 7.2 Hz). ^{13}C NMR (100 MHz, $CDCl_3$): δ 170.6, 164.6, 162.6, 155.6, 150.5, 147.7, 140.8, 131.1, 121.9, 120.4, 114.7, 111.5, 110.7, 68.0, 63.7, 56.1, 53.7, 46.7, 33.8, 31.0, 29.6, 29.3, 24.8, 24.2, 14.9. HRMS *m/z* (+EI) calcd for $C_{25}H_{29}N_3O_5$ $(M)^+$, 452.2180; found, 452.2180. HPLC purity = >98%, retention time = 6.10 min. Method B: purity = >98%, retention time = 3.13 min. Yield = 64%, 74 mg (over two steps), creamy white solid.

*(S)-4-((7-Methoxy-5-oxo-2,3,5,11a-tetrahydro-1H-benzo[e]-pyrrolo[1,2-a][1,4]diazepin-8-yl)oxy)-N-(4-methoxyphenyl)-butanamide (**20**).* ^{1}H NMR (400 MHz, $CDCl_3$): δ 7.67 (d, 1H, *J* = 4.4 Hz), 7.59 (s, 1H), 7.52 (s, 1H), 7.38 (dd, 2H, *J* = 2.0, 6.8 Hz), 6.88−6.63 (m, 3H), 4.23−4.10 (m, 2H), 3.87−3.77 (m, 1H), 3.88 (s, 3H), 3.79 (s, 3H), 3.75−3.68 (m, 1H), 3.61−3.55 (m, 1H), 2.62−2.58 (m, 2H), 2.33−2.25 (m, 4H), 2.10−2.00 (m, 2H). ^{13}C NMR (100 MHz, $CDCl_3$): δ 170.5, 164.6, 162.5, 156.3, 150.4, 147.6, 140.7, 131.0, 121.9, 120.5, 114.1. 111.6, 110.8, 67.9, 56.1, 55.5, 53.7, 46.7, 33.9, 31.0, 29.6, 29.3, 24.8, 24.2. HRMS *m/z* (+EI) calcd for $C_{24}H_{27}N_3O_5$ $(M)^+$, 438.2024; found, 438.2023. HPLC Method A: purity = >98%, retention time = 5.82 min. Method B: purity = >98%, retention time = 2.97 min. Yield = 61%, 68 mg (over two steps), creamy white solid.

*(S)-N-(4-Hydroxyphenyl)-4-((7-methoxy-5-oxo-2,3,5,11a-tetrahydro-1H-benzo[e]pyrrolo[1,2-a][1,4]diazepin-8-yl)oxy)butanamide (**21**).* ^{1}H NMR (400 MHz, $(CD_3)_2SO$): δ 9.70 (s, 1H), 9.15 (s, 1H), 7.78 (d, 1H, *J* = 4.4 Hz), 7.36 (dd, 2H, *J* = 2.0, 6.8 Hz), 7.33 (s, 1H), 6.84 (s, 1H), 6.67 (dd, 2H, *J* = 2.0, 6.8 Hz) 4.15−4.01 (m, 2H), 3.82 (s, 3H), 3.71−3.67 (m, 1H), 3.66−3.55 (m, 1H), 3.63−3.57 (m, 1H), 2.46−2.43 (m, 2H), 2.31−2.18 (m, 2H), 2.04−2.00 (m, 2H), 1.97−1.92 (m, 2H). ^{13}C NMR (100 MHz, $(CD_3)_2SO$): δ 169.8, 164.2, 163.3, 153.1, 150.2, 146.9, 140.5, 130.9, 120.8, 119.9, 119.7, 114.9, 111.1, 110.1, 68.5, 55.5, 46.3, 32.4, 32.1, 30.7, 28.8, 24.5, 23.6. HRMS *m/z* (+EI) calcd for $C_{23}H_{25}N_3O_5$ $(M)^+$, 424.1867; found, 424.1867. HPLC purity = >98%, retention time = 5.23 min. Method B: purity = >98%, retention time = 2.65 min. Yield = 57%, 61 mg (over two steps), creamy white solid.

*(S)-N-(3,4-Dimethylphenyl)-4-((7-methoxy-5-oxo-2,3,5,11a-tetrahydro-1H-benzo[e]pyrrolo[1,2-a][1,4]diazepin-8-yl)oxy)-butanamide (**22**).* ^{1}H NMR (400 MHz, $CDCl_3$): δ 7.60 (d, 1H, *J* = 4.4 Hz), 7.46 (s, 1H), 7.42 (s, 1H), 7.20 (s, 1H), 7.11 (dd, 1H, *J* = 1.6, 7.6 Hz), 6.98 (d, 1H, *J* = 8.0 Hz), 6.76 (s, 1H), 4.18−4.05 (m, 2H), 3.83 (s, 3H), 3.78−3.71 (m, 1H), 3.67−3.61 (m, 1H), 3.57−3.47 (m, 1H), 2.54−2.48 (m, 2H), 2.27−2.19 (m, 4H), 2.16 (s, 3H), 2.14 (s, 3H), 2.02−1.97 (m, 2H). ^{13}C NMR (100 MHz, $CDCl_3$): δ 170.5, 164.6, 162.5, 150.4, 147.7, 140.7, 137.2, 135.6, 132.6, 129.9, 121.4, 120.5, 117.5, 111.6, 110.9, 67.9, 56.1, 53.7, 46.7, 34.0, 29.6, 24.8, 24.2, 19.9, 19.2. HRMS *m/z* (+EI) calcd for $C_{25}H_{29}N_3O_4$ $(M)^+$, 436.2232; found, 436.2231. HPLC Method A: purity = >98%, retention time = 6.33 min. Method B: purity = >98%, retention time = 3.27 min. Yield = 64%, 71 mg (over two steps), creamy white solid.

*(S)-4-((7-Methoxy-5-oxo-2,3,5,11a-tetrahydro-1H-benzo[e]-pyrrolo[1,2-a][1,4]diazepin-8-yl)oxy)-N-(p-tolyl)butanamide (**23**).* ^{1}H NMR (400 MHz, $CDCl_3$): δ 7.68 (s, 1H), 7.59 (d, 1H, *J* = 4.4 Hz), 7.44 (s, 1H), 7.30 (d, 2H, *J* = 8.4 Hz), 7.03 (d, 2H, *J* = 8.4 Hz), 6.75 (s, 1H), 4.14−4.02 (m, 2H), 3.81 (s, 3H), 3.78−3.68 (m, 1H), 3.67−3.61 (m, 1H), 3.55−3.47 (m, 1H), 2.53−2.48 (m, 2H), 2.28−2.16 (m, 7H), 2.02−1.94 (m, 2H). ^{13}C NMR (100 MHz, $CDCl_3$): δ 170.6, 164.6, 162.5, 150.4, 147.7, 140.7, 135.4, 133.8, 129.4, 120.4, 120.0, 111.6, 110.8, 67.9, 56.1, 53.7, 46.7, 34.0, 31.0, 29.6, 29.3, 24.8, 24.2, 20.9. HRMS *m/z* (+EI) calcd for $C_{24}H_{27}N_3O_4$ $(M)^+$, 422.2074; found, 422.2074. HPLC Method A: purity = >98%, retention time = 6.22 min. Method B: purity = >98%, retention time = 3.17 min. Yield = 70%, 75 mg (over two steps), creamy white solid.

*(S)-4-((7-Methoxy-5-oxo-2,3,5,11a-tetrahydro-1H-benzo[e]-pyrrolo[1,2-a][1,4]diazepin-8-yl)oxy)-N-(m-tolyl)butanamide (**24**).* ^{1}H NMR (400 MHz, $CDCl_3$): δ 7.88 (s, 1H), 7.67 (d, 1H, *J* = 4.4 Hz), 7.52 (s, 1H), 7.38 (s, 1H), 7.28 (d, 1H, *J* = 8.0 Hz), 7.18 (t, 1H, *J* = 8.0 Hz), 6.91 (d, 1H, *J* = 7.2 Hz), 6.83 (s, 1H), 4.19−4.09 (m, 2H), 3.88 (s, 3H), 3.86−3.79 (m, 1H), 3.74−3.68 (m, 1H), 3.62−3.55 (m, 1H), 2.61−2.57 (m, 2H), 2.36−2.23 (s, 7H), 2.10−2.01 (m, 2H). ^{13}C NMR (100 MHz, $CDCl_3$): δ 170.7, 164.6, 162.6, 150.5, 147.7, 140.7, 138.8, 138.0, 128.7, 124.9, 120.6, 120.4, 117.0, 111.6, 110.8, 67.9, 56.1, 46.7, 34.0, 29.6, 29.3, 24.8, 24.2, 21.5. HRMS *m/z* (+EI) calcd for $C_{24}H_{27}N_3O_4$ $(M)^+$, 422.2074; found, 422.2074. HPLC Method A: purity = >98% retention time = 6.15 min. Method B: purity = >98%, retention time = 3.15 min. Yield = 68%, 73 mg (over two steps), creamy white solid.

*(S)-4-((7-Methoxy-5-oxo-2,3,5,11a-tetrahydro-1H-benzo[e]-pyrrolo[1,2-a][1,4]diazepin-8-yl)oxy)-N-phenylbutanamide (**25**).* ^{1}H NMR (400 MHz, $CDCl_3$): δ 7.80 (s, 1H), 7.65 (d, 1H, *J* = 4.4 Hz), 7.50 (s, 1H), 7.49 (d, 2H, *J* = 8.0 Hz), 7.29 (t, 2H, *J* = 8.0 Hz), 7.07 (t, 1H, *J* = 7.6 Hz), 6.81 (s, 1H), 4.19−4.08 (m, 2H), 3.86 (s, 3H), 3.84−3.77 (m, 1H), 3.72−3.67 (m, 1H), 3.60−3.53 (m, 1H), 2.62−2.58 (m, 2H), 2.31−2.24 (m, 4H), 2.10−2.00 (m, 2H). ^{13}C NMR (100 MHz, $CDCl_3$): δ 170.7, 164.6, 16.6, 150.4, 147.7, 140.7, 138.0, 129.0, 124.2, 124.5, 119.9, 111.6, 110.8, 67.9, 56.1, 53.7, 53.5, 46.7, 34.05, 29.6, 29.3, 24.8, 24.2. HRMS *m/z* (+EI) calcd for $C_{23}H_{25}N_3O_4$ $(M)^+$, 408.1918; found, 408.1918. HPLC Method A: purity = >98%, retention time = 5.93 min. Method B: purity = >98%, retention time = 3.00 min. Yield = 70%, 73 mg (over two steps), creamy white solid.

*(S)-4-((7-Methoxy-5-oxo-2,3,5,11a-tetrahydro-1H-benzo[e]-pyrrolo[1,2-a][1,4]diazepin-8-yl)oxy)-N-(pyridin-3-yl)butanamide (**26**).* ^{1}H NMR (400 MHz, $CDCl_3$): δ 8.82 (s, 1H), 8.51 (d, 1H, *J* = 2.4 Hz), 8.23 (dd, 1H, *J* = 1.2, 4.8 Hz), 8.14 (d, 1H, *J* = 7.6 Hz) 7.59 (d, 1H, *J* = 4.4 Hz), 7.41 (s, 1H), 7.18 (dd, 1H, *J* = 4.8, 8.4 Hz), 6.74 (s, 1H), 4.05−4.01 (m, 2H), 3.78−3.71 (m, 4H), 3.66−6.61 (m, 1H), 3.52−3.47 (m, 1H), 2.54−2.51 (m, 2H), 2.26−2.24 (m, 2H), 2.19−2.15 (m, 2H), 2.02−1.95 (m, 2H). ^{13}C NMR (100 MHz, $CDCl_3$): δ 171.6, 164.6, 162.7, 150.4, 147.6, 144.7, 141.2, 140.7, 135.4, 127.2, 123.6, 120.3, 111.6, 110.6, 67.9, 56.0, 53.8, 46.7, 33.7, 29.5, 24.7, 24.2. HRMS *m/z* (+EI) calcd for $C_{22}H_{24}N_4O_4$ $(M)^+$, 409.1870; found, 409.1866. HPLC Method A: purity = >98%, retention time = 4.67 min. Method B: purity = >98%, retention time = 2.35 min. Yield = 56%, 58 mg (over two steps), creamy white solid.

*(S)-4-((7-Methoxy-5-oxo-2,3,5,11a-tetrahydro-1H-benzo[e]-pyrrolo[1,2-a][1,4]diazepin-8-yl)oxy)-N-(pyridin-4-yl)butanamide (**27**).* ^{1}H NMR (400 MHz, $CDCl_3$): δ 8.95 (s, 1H), 8.41 (d, 2H, *J* = 6.0 Hz), 7.64 (d, 1H, *J* = 4.4 Hz), 7.49 (dd, 2H, *J* = 1.6. 6.4 Hz), 7.46 (s, 1H), 6.79 (s, 1H), 4.10−4.06 (m, 2H), 3.81 (s, 3H), 3.79−3.76 (m, 1H), 3.71−3.67 (m, 1H), 3.57−3.52 (m, 1H), 2.60−2.56 (m,

DOI: 10.1021/acs.jmedchem.8b01849
J. Med. Chem. 2019, 62, 2127−2139

2H), 2.32−2.29 (m, 2H), 2.23 (t, 2H, J = 6.4 Hz), 2.07−1.99 (m, 2H).). ^{13}C NMR (100 MHz, $CDCl_3$): δ 171.8, 164.6, 162.7, 150.4, 150.3, 147.6, 145.6, 140.7, 120.4, 113.6, 111.6, 110.7, 67.8, 56.0, 53.5, 46.7, 34.0, 29.7, 24.5, 24.2. HRMS m/z (+EI) calcd for $C_{22}H_{24}N_4O_4$ $(M)^+$, 409.1870; found, 409.1866. HPLC Method A: purity = >98%, retention time = 4.06 min. Method B: purity = >98%, retention time = 2.40 min. Yield = 58%, 60 mg (over two steps), creamy white solid.

*(S)-N-Cyclohexyl-4-((7-methoxy-5-oxo-2,3,5,11a-tetrahydro-1H-benzo[e]pyrrolo[1,2-a][1,4]diazepin-8-yl)oxy)butanamide (**28**).* ^{1}H NMR (400 MHz, $CDCl_3$): δ 7.65 (d, 1H, J = 4.4 Hz), 7.50 (s, 1H), 6.80 (s, 1H) 5.54 (d, 1H, J = 4.0 Hz), 4.14−4.03 (m, 2H), 3.93 (s, 1H), 3.83−3.76 (m, 1H), 3.76−3.67 (m, 2H), 3.59−3.51 (m, 1H), 2.36 (t, 2H, J = 7.6 Hz), 2.38−2.32 (m, 2H), 2.33−2.28 (m, 2H), 2.20−2.15 (m, 2H), 2.08−2.01 (m, 2H), 1.84−1.80 (m, 3H), 1.67−1.55 (m, 3H), 1.39−1.24 (m, 2H), 1.13−0.97 (m, 2H). ^{13}C NMR (100 MHz, $CDCl_3$): δ 171.1, 164.6, 162.5, 150.6, 147.7, 140.8, 120.4, 111.6, 110.8, 67.9, 56.1, 53.7, 48.1, 46.7, 33.2, 31.8, 31.0, 29.6, 29.3, 25.6, 25.0, 24.9, 24.2. HRMS m/z (+EI) calcd for $C_{23}H_{31}N_3O_4$ $(M)^+$, 414.2389; found, 414.2387. HPLC Method A: purity = 93%, retention time = 5.80 min. Method B: purity = 94%, retention time = 3.00 min. Yield = 64%, 67 mg (over two steps), orange oil.

*(S)-N-Butyl-4-((7-methoxy-5-oxo-2,3,5,11a-tetrahydro-1H-benzo[e]pyrrolo[1,2-a][1,4]diazepin-8-yl)oxy)butanamide (**29**).* ^{1}H NMR (400 MHz, $CDCl_3$): δ 7.65 (d, 1H, J = 4.4 Hz), 7.49 (s, 1H), 6.79 (s, 1H), 5.95 (bs, 1H), 4.13−4.03 (m, 2H), 3.91 (s, 3H), 3.83−3.77 (m, 1H), 3.71−3.67 (m, 1H), 3.59−3.52 (m, 1H), 3.23−3.18 (m, 2H), 2.40−2.36 (m, 2H), 2.32−2.29 (m, 2H), 2.18−2.13 (m, 2H), 2.08−2.01 (m, 2H), 1.46−1.39 (m, 2H), 1.34−1.26 (m, 2H), 0.87 (t, 3H, J = 7.2 Hz). ^{13}C NMR (100 MHz, $CDCl_3$): δ 172.2, 164.6, 162.5, 150.5, 147.7, 140.7, 120.3, 111.5, 110.7, 68.0, 56.1, 53.8, 46.7, 39.3, 33.0, 31.8, 29.6, 24.9, 24.2, 20.1, 13.8. HRMS m/z (+EI) calcd for $C_{21}H_{29}N_3O_4$ $(M)^+$, 388.2231; found, 388.2224. HPLC Method A: purity = >98%, retention time = 5.57 min. Method B: purity = >98%, retention time = 2.85 min. Yield = 73%, 72 mg (over two steps), orange oil.

*(S)-4-((7-Methoxy-5-oxo-2,3,5,11a-tetrahydro-1H-benzo[e]-pyrrolo[1,2-a][1,4]diazepin-8-yl)oxy)-N-propylbutanamide (**30**).* ^{1}H NMR (400 MHz, $CDCl_3$): δ 7.66 (d, 1H, J = 4.4 Hz), 7.50 (s, 1H), 6.81 (s, 1H), 5.96 (bs, 1H), 4.15−4.04 (m, 2H), 3.91 (s, 3H), 3.84−3.78 (m, 1H), 3.72−3.68 (m, 1H), 3.60−3.57 (m, 1H), 3.21−3.16 (m, 2H), 2.40−2.38 (m, 2H), 2.36−2.23 (m, 2H), 2.21−2.16 (m, 2H), 2.09−2.01 (m, 2H), 1.47 (sex, 2H, J = 7.2 Hz), 0.87 (t, 3H, J = 4.0 Hz). ^{13}C NMR (100 MHz, $CDCl_3$): δ 172.2, 164.6, 162.5,, 150.5, 147.7, 140.7, 120.3, 111.5, 110.7, 68.0, 56.1, 46.7, 41.2, 33.0, 29.6, 29.3, 25.0, 24.2, 22.9, 11.4. HRMS m/z (+EI) calcd for $C_{20}H_{27}N_3O_4$ $(M)^+$, 374.2074; found, 374.2071. HPLC Method A: purity = >98%, retention time = 5.33 min. Method B: purity = >98%, retention time = 2.68 min. Yield = 64%, 61 mg (over two steps), orange oil.

*(S)-N-Ethyl-4-((7-methoxy-5-oxo-2,3,5,11a-tetrahydro-1H-benzo[e]pyrrolo[1,2-a][1,4]diazepin-8-yl)oxy)butanamide (**31**).* ^{1}H NMR (400 MHz, $CDCl_3$): δ 7.65 (d, 1H, J = 4.4 Hz), 7.49 (s, 1H), 6.80 (s, 1H), 5.98 (bs, 1H), 4.14−4.04 (m, 2H), 3.92 (s, 3H), 3.83−3.77 (m, 1H), 3.72−3.69 (m, 1H), 3.59−3.52 (m, 1H), 3.29−3.22 (m, 2H), 2.41−2.34 (m, 2H), 2.32−2.30 (m, 2H), 2.20−2.14 (m, 2H), 2.10−1.99 (m, 2H), 1.08 (t, 3H, J = 7.2 Hz). ^{13}C NMR (100 MHz, $CDCl_3$): δ 172.1, 164.6, 162.5, 150.5, 147.7, 140.7, 120.3, 111.5, 110.7, 68.0, 56.1, 46.7, 34.3, 33.0, 29.6, 29.3, 24.9, 24.2, 14.8. HRMS m/z (+EI) calcd for $C_{19}H_{25}N_3O_4$ $(M)^+$, 360.1918; found, 360.1913. HPLC Method A: purity = >98%, retention time = 5.08 min. Method B: purity = >98%, retention time = 2.55 min. Yield = 67%, 61 mg (over two steps), orange oil.

*(S)-4-((7-Methoxy-5-oxo-2,3,5,11a-tetrahydro-1H-benzo[e]-pyrrolo[1,2-a][1,4]diazepin-8-yl)oxy)-N-methylbutanamide (**32**).* ^{1}H NMR (400 MHz, $CDCl_3$): δ 7.60 (d, 1H, J = 4.4 Hz), 7.44 (s, 1H), 6.74 (s, 1H), 5.98 (bs, 1H), 4.09−3.98 (m, 2H), 3.87 (s, 3H), 3.78−3.72 (m, 3H), 3.66−3.63 (m, 1H), 3.54−3.47 (m, 1H), 2.73 (d, 3H, J = 4.8 Hz), 2.35−2.33 (m, 2H), 2.29−2.23 (m, 2H), 2.02−1.94 (m, 2H). ^{13}C NMR (100 MHz, $CDCl_3$): δ 172.9, 164.6, 162.5, 150.5, 147.6, 140.7, 120.4, 111.6, 110.6, 68.1, 56.1, 53.7, 46.7, 33.0, 29.6, 26.3, 24.9, 24.2. HRMS m/z (+EI) calcd for $C_{18}H_{23}N_3O_4$ $(M)^+$, 346.1761; found, 346.1757. HPLC Method A: purity = >98%, retention time = 4.88 min. Method B: purity = >98%, retention time = 2.47 min. Yield = 69%, 60 mg (over two steps), orange oil.

Primary CLL, JJN-3 and Healthy B and T Cell Cytotoxicity Screening. Primary CLL cells and primary B and T cells were obtained from patient/healthy donor blood samples using density gradient centrifugation with Histopaque and were phenotyped for CD3, CD5 and CD19 using an Accuri C6 flow cytometer. The primary cells were used within 24 h of sample preparation and were maintained in Roswell Park Memorial Institute (RPMI) media (10% foetal bovine serum (FBS), 1% glutamate and 1% pen/strep. IL-4 was also added to primary CLL cell cultures alongside treatment with test compounds at a concentration of 5 ng/mL.

JJN-3 cells were maintained in Dulbecco's modified Eagle's media containing 20% FBS, 1% pen/strep, and 1% pyruvate at concentrations between 500 000 and 2 000 000 cells/mL. All cells were maintained at 37 °C in atmospheric conditions of 5% CO_2.

Cytotoxicity screenings were carried out in triplicate with these cells at a cell density of 1 000 000 cells/mL. Cells were treated with test compounds at a range of concentrations to establish LC_{50} values. Cells were incubated with the compounds for 48 h before being harvested. annexin V/PI positivity was then determined using the annexin V apoptosis detection kit (eBioscience) in accordance with the manufacturer's instructions. Following staining with FITC labeled annexin V and propidium iodide, samples were analyzed on the Accuri C6 flow cytometer to determine relative levels of cell death in the sample. Prism 6 software was then used to analyze the data to obtain dose−response curves.

Nuclear NF-κB (ELISA) Assay. 5 000 000 JJN-3 cells were treated for 4 h with test compounds alongside untreated controls before being harvested and spun down. Nuclear extracts were then produced using the nuclear extraction kit purchased from Active Motif. Nuclear extracts were stored at −80 °C before use in the NF-kB family ELISA kit (Active Motif). Total protein levels in the nuclear extracts were determined using a BCA protein detection kit, which allowed the calculation of nuclear extract volume equivalent to 1 μg of total protein. This was then added in accordance with the manufacturer's instructions to the ELISA plate. An optical density reading of the plate at 450 nm was then recorded. The sample absorbance values were then normalized with the standard curve absorbance values obtained from recombinant NF-κB subunit protein purchased from Active Motif. This allowed the calculation of the concentration of each NF-κB subunit present in the nuclear extract following treatment, compared with an untreated control.

Molecular Modeling. Double-stranded DNA type B was generated by the NAB module of AMBER 16.0 package program, using the template of the sequences used in the study. The PDB file for the ligands was generated by ChemOffice 16.0. All of the DNA and ligand structures were minimized by SYBYL software before molecular docking. Molecular docking of the ligands to each of the generated DNA sequences was performed using the SMINA molecular docking program. All parameters were kept at their default values. The grid box was prepared to cover the full length of the DNA to allow the ligand molecules to explore all the possible binding sites of DNA including the major grooves and minor grooves.

■ ASSOCIATED CONTENT

Supporting Information

The Supporting Information is available free of charge on the ACS Publications website at DOI: 10.1021/acs.jmedchem.8b01849.

Synthesis of PBD Core **10**; NMR spectra and HRMS; docking poses of selected compounds, additional QSAR data; cellular kill curves for the primary CLL; JJN-3 cell line and healthy B- and T-cell cytotoxicity evaluations (PDF)

PDB files for AT-rich and GC-rich DNA sequences (ZIP)

DOI: 10.1021/acs.jmedchem.8b01849
J. Med. Chem. 2019, 62, 2127−2139

Molecular formula strings (CSV)

AUTHOR INFORMATION

Corresponding Authors

*E-mail: david.thurston@kcl.ac.uk. Phone: (+44) 7973 801535 (D.E.T.).

*E-mail: k.miraz.rahman@kcl.ac.uk. Phone: (+44) 207 848 1891 (K.M.R.).

ORCID

Khondaker Miraz. Rahman: 0000-0001-8566-8648

Notes

The authors declare the following competing financial interest(s): K.M.R. and D.E.T. are both shareholders in Transcriptogen Ltd and Femtogenix Ltd, which work in the area of DNA-interactive molecules.

ACKNOWLEDGMENTS

This work was supported by a grant (12-1263/JGATCBR) from Worldwide Cancer Research (WCR; formerly AICR) to D.E.T., K.M.R. and CP (2012). WCR is also thanked for a PhD studentship to D.B.C.

ABBREVIATIONS

ADC, antibody−drug conjugate; Alloc, allyloxycarbonyl;; CLL, chronic lymphocytic leukaemia; ELISA, enzyme-linked immunosorbent assay; LC−MS, liquid chromatography−mass spectrometry; NF-κB, nuclear factor kappa B; NF-Y, nuclear transcription factor Y; PBD, pyrrolo[2,1-*c*][1,4]-benzodiazepine; PDB, protein data bank; QSAR, quantitative structure−activity relationship; THP, tetrahydropyran

REFERENCES

(1) Puvvada, M. S.; Hartley, J. A.; Jenkins, T. C.; Thurston, D. E. A quantitative assay to measure the relative DNA-binding affinity of pyrrolo[2,1-C][1,4]benzodizepine (PBD) antitumour antibiotics based on the inhibition of restriction endonuclease BAMHI. *Nucleic Acids Res.* **1993**, *21*, 3671−3675.

(2) Wells, G.; Martin, C. R. H.; Howard, P. W.; Sands, Z. A.; Laughton, C. A.; Tiberghien, A.; Woo, C. K.; Masterson, L. A.; Stephenson, M. J.; Hartley, J. A.; Jenkins, T. C.; Shnyder, S. D.; Loadman, P. M.; Waring, M. J.; Thurston, D. E. Design, synthesis, and biophysical and biological evaluation of a series of pyrrolobenzodiazepine - poly(N-methylpyrrole) conjugates−Poly(N-methylpyrrole) Conjugates. *J. Med. Chem.* **2006**, *49*, 5442−5461.

(3) Puvvada, M. S.; Forrow, S. A.; Hartley, J. A.; Stephenson, P.; Gibson, I.; Jenkins, T. C.; Thurston, D. E. Inhibition of bacteriophage T7 RNA polymerase in vitro transcription by DNA-binding pyrrolo[2,1-c][1,4]benzodiazepines. *Biochemistry* **1997**, *36*, 2478−2484.

(4) Gerratana, B. Biosynthesis, synthesis, and biological activities of pyrrolobenzodiazepines. *Med. Res. Rev.* **2010**, *32*, 254−293.

(5) Hurley, L. H.; Reck, T.; Thurston, D. E.; Langley, D. R.; Holden, K. G.; Hertzberg, R. P.; Hoover, J. R. E.; Gallagher, G., Jr; Faucette, L. F. Pyrrolo [1, 4] benzodiazepine antitumor antibiotics: relationship of DNA alkylation and sequence specificity to the biological activity of natural and synthetic compounds. *Chem. Res. Toxicol.* **1988**, *1*, 258−268.

(6) Cheatham, S.; Kook, A.; Hurley, L. H.; Barkley, M. D.; Remers, W. One-and two-dimensional proton NMR, fluorescence and molecular modeling studies on the tomaymycin-d (ATGCAT) 2 adduct. Evidence for two covalent adducts with opposite orientations and stereochemistries at the covalent linkage site. *J. Med. Chem.* **1988**, *31*, 583−590.

(7) Graves, D. E.; Pattaroni, C.; Krishnan, B. S.; Ostrander, J. M.; Hurley, L. H.; Krugh, T. R. The reaction of anthramycin with DNA. Proton and carbon nuclear magnetic resonance studies on the structure of the anthramycin-DNA adduct. *J Biol Chem.* **1984**, *259*, 8202.

(8) Hurley, L. H.; Petrusek, R. Proposed structure of the anthramycin−DNA adduct. *Nature* **1979**, *282*, 529−531.

(9) Hertzberg, R. P.; Hecht, S. M.; Reynolds, V. L.; Molineux, I. J.; Hurley, L. H. DNA sequence specificity of the pyrrolo [1, 4] benzodiazepine antitumor antibiotics. Methidiumpropyl-EDTA-iron (II) footprinting analysis of DNA binding sites for anthramycin and related drugs. *Biochemistry* **1986**, *25*, 1249−1258.

(10) Rahman, K. M.; Vassoler, H.; James, C. H.; Thurston, D. E. DNA sequence preference and adduct orientation of pyrrolo [2, 1-c][1, 4] benzodiazepine antitumor agents. *ACS Med. Chem. Lett.* **2010**, *1*, 427−432.

(11) Darnell, J. E. Transcription factors as targets for cancer therapy. *Nat. Rev. Cancer* **2002**, *2*, 740−749.

(12) Kordes, U.; Krappmann, D.; Heissmeyer, V.; Ludwig, W.; Scheidereit, C. Transcription factor NF-[kappa] B is constitutively activated in acute lymphoblastic leukemia cells. *Leukemia* **2000**, *14*, 399.

(13) Nishio, M.; Endo, T.; Tsukada, N.; Ohata, J.; Kitada, S.; Reed, J. C.; Zvaifler, N. J.; Kipps, T. J. Nurselike cells express BAFF and APRIL, which can promote survival of chronic lymphocytic leukemia cells via a paracrine pathway distinct from that of SDF-1α. *Blood* **2005**, *106*, 1012−1020.

(14) Guzman, M. L.; Neering, S. J.; Upchurch, D.; Grimes, B.; Howard, D. S.; Rizzieri, D. A.; Luger, S. M.; Jordan, C. T. Nuclear factor-κB is constitutively activated in primitive human acute myelogenous leukemia cells. *Blood* **2001**, *98*, 2301−2307.

(15) Grandage, V. L.; Gale, R. E.; Linch, D. C.; Khwaja, A. PI3-kinase/Akt is constitutively active in primary acute myeloid leukaemia cells and regulates survival and chemoresistance via NF-kB, MAPkinase and p53 pathways. *Leukemia* **2005**, *19*, 586−594.

(16) Kotecha, M.; Kluza, J.; Wells, G.; O'Hare, C. C.; Forni, C.; Mantovani, R.; Howard, P. W.; Morris, P.; Thurston, D. E.; Hartley, J. A.; Hochhauser, D. Inhibition of DNA binding of the NF-Y transcription factor by the pyrrolobenzodiazepine-polyamide conjugate GWL-78. *Mol. Cancer Ther.* **2008**, *7*, 1319−1328.

(17) Hu, W.-P.; Tsai, F.-Y.; Yu, H.-S.; Sung, P.-J.; Chang, L.-S.; Wang, J.-J. Induction of apoptosis by DC-81-indole conjugate agent through NF-κB and JNK/AP-1 pathway. *Chem. Res. Toxicol.* **2008**, *21*, 1330−1336.

(18) Rahman, K. M.; Jackson, P. J. M.; James, C. H.; Basu, B. P.; Hartley, J. A.; de la Fuente, M.; Schatzlein, A.; Robson, M.; Pedley, R. B.; Pepper, C.; Fox, K. R.; Howard, P. W.; Thurston, D. E. GC-targeted C8-linked pyrrolobenzodiazepine−biaryl conjugates with femtomolar in vitro cytotoxicity and in vivo antitumor activity in mouse models. *J. Med. Chem.* **2013**, *56*, 2911−2935.

(19) Rahman, K. M.; Rosado, H.; Moreira, J. B.; Feuerbaum, E.-A.; Fox, K. R.; Stecher, E.; Howard, P. W.; Gregson, S. J.; James, C. H.; de la Fuente, M.; Waldron, D. E.; Thurston, D. E.; Taylor, P. W. Antistaphylococcal activity of DNA-interactive pyrrolobenzodiazepine (PBD) dimers and PBD-biaryl conjugates. *J. Antimicrob. Chemother.* **2012**, *67*, 1683−1696.

(20) Andriollo, P.; Hind, C. K.; Picconi, P.; Nahar, K. S.; Jamshidi, S.; Varsha, A.; Clifford, M.; Sutton, J. M.; Rahman, K. M. C8-linked pyrrolobenzodiazepine monomers with inverted building blocks show selective activity against multidrug resistant Gram-positive bacteria. *ACS Infect. Dis.* **2018**, *4*, 158−174.

(21) Brucoli, F.; Guzman, J. D.; Basher, M. A.; Evangelopoulos, D.; McMahon, E.; Munshi, T.; McHugh, T. D.; Fox, K. R.; Bhakta, S. DNA sequence-selective C8-linked pyrrolobenzodiazepine−heterocyclic polyamide conjugates show anti-tubercular-specific activities. *J. Antibiot.* **2016**, *69*, 843.

(22) Mantaj, J.; Jackson, P. J. M.; Rahman, K. M.; Thurston, D. E. From anthramycin to pyrrolobenzodiazepine (PBD)-containing antibody−drug conjugates (ADCs). *Angew. Chem., Int. Ed.* **2016**, *56*, 462−488.

DOI: 10.1021/acs.jmedchem.8b01849
J. Med. Chem. 2019, 62, 2127−2139

(23) Hsieh, M.-C.; Hu, W.-P.; Yu, H.-S.; Wu, W.-C.; Chang, L.-S.; Kao, Y.-H.; Wang, J.-J. A DC-81-indole conjugate agent suppresses melanoma A375 cell migration partially via interrupting VEGF production and stromal cell-derived factor-1α-mediated signaling. *Toxicol. Appl. Pharmacol.* **2011**, *255*, 150−159.
(24) Hu, W.-P.; Yu, H.-S.; Sung, P.-J.; Tsai, F.-Y.; Shen, Y.-K.; Chang, L.-S.; Wang, J.-J. DC-81-indole conjugate agent induces mitochondria mediated apoptosis in human melanoma A375 cells. *Chem. Res. Toxicol.* **2007**, *20*, 905−912.
(25) Boger, D. L.; Fink, B. E.; Hedrick, M. P. Total synthesis of distamycin A and 2640 analogues: a solution-phase combinatorial approach to the discovery of new, bioactive DNA binding agents and development of a rapid, high-throughput screen for determining relative DNA binding affinity or DNA binding sequence selectivity. *J. Am. Chem. Soc.* **2000**, *122*, 6382−6394.
(26) Boger, D. L.; Schmitt, H. W.; Fink, B. E.; Hedrick, M. P. Parallel synthesis and evaluation of 132 (+)-1, 2, 9, 9a-tetrahydrocyclopropa [c] benz [e] indol-4-one (CBI) analogues of CC-1065 and the duocarmycins defining the contribution of the DNA-binding domain. *J. Org. Chem.* **2001**, *66*, 6654−6661.
(27) Basher, M. A.; Rahman, K. M.; Jackson, P. J. M.; Thurston, D. E.; Fox, K. R. Sequence-selective binding of C8-conjugated pyrrolobenzodiazepines (PBDs) to DNA. *Biophys. Chem.* **2017**, *230*, 53−61.
(28) Hewamana, S.; Alghazal, S.; Lin, T. T.; Clement, M.; Jenkins, C.; Guzman, M. L.; Jordan, C. T.; Neelakantan, S.; Crooks, P. A.; Burnett, A. K.; Pratt, G.; Fegan, C.; Rowntree, C.; Brennan, P.; Pepper, C. The NF-κB subunit Rel A is associated with in vitro survival and clinical disease progression in chronic lymphocytic leukemia and represents a promising therapeutic target. *Blood* **2008**, *111*, 4681−4689.
(29) Endo, T.; Nishio, M.; Enzler, T.; Cottam, H. B.; Fukuda, T.; James, D. F.; Karin, M.; Kipps, T. J. BAFF and APRIL support chronic lymphocytic leukemia B-cell survival through activation of the canonical NF-κB pathway. *Blood* **2007**, *109*, 703−710.
(30) Herishanu, Y.; Perez-Galan, P.; Liu, D.; Biancotto, A.; Pittaluga, S.; Vire, B.; Gibellini, F.; Njuguna, N.; Lee, E.; Stennett, L.; Raghavachari, N.; Liu, P.; McCoy, J. P.; Raffeld, M.; Stetler-Stevenson, M.; Yuan, C.; Sherry, R.; Arthur, D. C.; Maric, I.; White, T.; Marti, G. E.; Munson, P.; Wilson, W. H.; Wiestner, A. The lymph node microenvironment promotes B-cell receptor signaling, NF-êB activation, and tumor proliferation in chronic lymphocytic leukemia. *Blood* **2010**, *117*, 563−574.
(31) Mitsiades, C. S.; Mitsiades, N.; Poulaki, V.; Schlossman, R.; Akiyama, M.; Chauhan, D.; Hideshima, T.; Treon, S. P.; Munshi, N. C.; Richardson, P. G.; Anderson, K. C. Activation of NF-[kappa] B and upregulation of intracellular anti-apoptotic proteins via the IGF-1/Akt signaling in human multiple myeloma cells: therapeutic implications. *Oncogene* **2002**, *21*, 5673.
(32) Ni, H.; Ergin, M.; Huang, Q.; Qin, J.-Z.; Amin, H. M.; Martinez, R. L.; Saeed, S.; Barton, K.; Alkan, S. Analysis of expression of nuclear factor κB (NF-κB) in multiple myeloma: downregulation of NF-κB induces apoptosis. *Br. J. Haematol.* **2001**, *115*, 279−286.
(33) Demchenko, Y. N.; Glebov, O. K.; Zingone, A.; Keats, J. J.; Bergsagel, P. L.; Kuehl, W. M. Classical and/or alternative NF-κB pathway activation in multiple myeloma. *Blood* **2010**, *115*, 3541−3552.
(34) Thurston, D. E.; Bose, D. S.; Howard, P. W.; Jenkins, T. C.; Leoni, A.; Baraldi, P. G.; Guiotto, A.; Cacciari, B.; Kelland, L. R.; Foloppe, M.-P.; Rault, S. Effect of A-ring modifications on the DNA-binding behavior and cytotoxicity of pyrrolo [2, 1-c][1, 4] benzodiazepines. *J. Med. Chem.* **1999**, *42*, 1951−1964.
(35) Borgatti, M.; Rutigliano, C.; Bianchi, N.; Mischiati, C.; Baraldi, P. G.; Romagnoli, R.; Gambari, R. Inhibition of NF-kB/DNA interactions and HIV-1 LTR directed transcription by hybrid molecules containing pyrrolo [2, 1-c][1, 4] benzodiazepine (PBD) and oligopyrrole carriers. *Drug Dev. Res.* **2003**, *60*, 173−185.
(36) Hewamana, S.; Lin, T. T.; Rowntree, C.; Karunanithi, K.; Pratt, G.; Hills, R.; Fegan, C.; Brennan, P.; Pepper, C. Rel a is an independent biomarker of clinical outcome in chronic lymphocytic leukemia. *J. Clin. Oncol.* **2009**, *27*, 763−769.
(37) Yu, Y.; Wan, Y.; Huang, C. The Biological Functions of NF-κB1 (p) and its Potential as an Anti-Cancer Target. *Curr. Cancer Drug Targets* **2009**, *9*, 566−571.
(38) Song, L.; Li, J.; Zhang, D.; Liu, Z.-g.; Ye, J.; Zhan, Q.; Shen, H.-M.; Whiteman, M.; Huang, C. IKKβ programs to turn on the GADD45α−MKK4−JNK apoptotic cascade specifically via p50 NF-κB in arsenite response. *J. Cell Biol.* **2006**, *175*, 607−617.
(39) Lee, C.-H.; Hu, W.-P.; Hong, C.-H.; Yu, H.-S.; Liao, W.-T.; Chen, C.-Y.; Chen, Y.-L.; Chen, B.-H.; Chen, G.-S.; Wang, J.-J. Pyrrolo [2, 1-c][1, 4] benzodiazepine and indole conjugate (IN6CPBD) has better efficacy and superior safety than the mother compound DC-81 in suppressing the growth of established melanoma in vivo. *Chem.-Biol. Interact.* **2009**, *180*, 360−367.

DOI: 10.1021/acs.jmedchem.8b01849
J. Med. Chem. 2019, 62, 2127−2139